Z. Zhang. Feature-based facial expression recognition: Sensitivity analysis and experiments with a multilayer perceptron.
International Journal of Pattern Recognition and Artificial Intelligence 13(6):893-911, 1999.

Feature-Based Facial Expression Recognition: Sensitivity Analysis and Experiments With a Multi-Layer Perceptron

Zhengyou Zhang

Microsoft Research

One Microsoft Way

Redmond WA 98052, USA

E-mail: `zhang@microsoft.com`

Running head: Feature-Based Facial Expression Recognition: Sensitivity Analysis

To appear in *International Journal of Pattern Recognition and Artificial Interlligence* (IJPRAI)

(accepted in 1998)

This article is the combined and revised version of the following two conference papers:

- Z. Zhang, M. Lyons. M. Schuster, and S. Akamatsu, "Comparison between geometry-based and Gabor-wavelets-based facial expression recognition uaing multi-layer perceptron", in *Proc. IEEE 3rd Int'l Conf. on Automatic Face and Gesture Recognition*, Nara, Japan, April 1998.
- Z. Zhang, "Feature-based facial expression recognition: sensitivity analysis", in *Proc. Post-ECCV Workshop on Advances in Facial Image Analysis and Recognition Technology*, Freiburg, Germany, June 1998.

Feature-Based Facial Expression Recognition: Sensitivity Analysis and Experiments With a Multi-Layer Perceptron

Zhengyou Zhang

Abstract

In this paper, we report our experiments on feature-based facial expression recognition within an architecture based on a two-layer perceptron. We investigate the use of two types of features extracted from face images: the geometric positions of a set of fiducial points on a face, and a set of multi-scale and multi-orientation Gabor wavelet coefficients at these points. They can be used either independently or jointly. The recognition performance with different types of features has been compared, which shows that Gabor wavelet coefficients are much more powerful than geometric positions. Furthermore, since the first layer of the perceptron actually performs a nonlinear reduction of the dimensionality of the feature space, we have also studied the desired number of hidden units, i.e., the appropriate dimension to represent a facial expression in order to achieve a good recognition rate. It turns out that five to seven hidden units are probably enough to represent the space of feature expressions. Then, we have investigated the importance of each individual fiducial point to facial expression recognition. Sensitivity analysis reveals that points on cheeks and on forehead carry little useful information. After discarding them, not only the computational efficiency increases, but also the generalization performance slightly improves. Finally, we have studied the significance of image scales. Experiments show that facial expression recognition is mainly a low frequency process, and a spatial resolution of 64 pixels $\times$ 64 pixels is probably enough.

Keywords: Facial expression recognition, learning, Gabor wavelets, multilayer perceptron, sensitivity analysis, image scale.

1. Introduction

There are a number of difficulties in facial expression recognition (FER) due to the variation of facial expression across the human population and to the context-dependent variation even for the same individual. Even we human beings may make mistakes [9]. On the other hand, FER by computer is very useful in many applications such as human behavior interpretation and human-computer interface.

An automatic FER system needs to solve the following problems: detection and location of faces in a cluttered scene, facial feature extraction, and facial expression classification.

Face detection has been studied by many researchers, and it seems that most successful systems are based on neural networks [24, 22]. Once a face is detected in the image, the corresponding region is extracted, and is usually normalized to have the same size (for example, the same distance between two eyes) and the same gray level. In this paper, we do not address the face detection problem.

Facial feature extraction attempts to find the most appropriate representation of the face images for recognition. There are mainly two approaches: holistic template-matching systems and geometric feature-based systems [4]. In holistic systems, a template can be a pixel image or a feature vector obtained after processing the face image as a whole. In the latter, principal component analysis and multilayer neural networks are extensively used to obtain a low-dimensional representation. In geometric feature-based systems, major face components and/or feature points are detected in the images. The distances between feature points and the relative sizes of the major face components are computed to form a feature vector. The feature points can also form a geometric graph representation of the faces. Feature-based techniques are usually computationally more expensive than template-based techniques, but are more robust to variation in scale, size, head orientation, and location of the face in an image. The work to be described in this paper is, to some extent, an hybrid approach. We first locate a set of feature points, and then extract a set of Gabor wavelet coefficients at each point through image convolution.

Compared with face recognition, there is relatively a small amount of work on facial expression recognition. The first category of previous work uses image sequences. Suwa et al. [23] did a preliminary analysis of facial expressions by tracking the motion of twenty identified spots. Mase [17] uses the means and variances of optical flow data at evenly divided small blocks. Yacoob and Davis [28] use the inter-frame motion of edges extracted in the area of the mouth, nose, eyes, and eyebrows. Bartlett et al. [2] use the combination of optical flow and principal components obtained from image differences. Essa and Pentland [10] builds a dynamic parametric model by tracking facial motion over time, which can then be used for analyzing facial expressions. The second category of previous work tries to classify facial expressions from static images. Turk and Pentland [26] represent face images by eigenfaces through linear principal component analysis. Padgett and Cottrell [19] use an approach similar to eigenfaces but with seven pixel blocks from feature regions (both eyes and mouth). Cottrell and Metcalfe [5] use holistic representations based on principal components, extracted by feed forward networks. Rahardja et al. [20] also use holistic representations with neural networks, but the images are represented in a pyramid structure. Lanitis et al. [14] use parameterized deformable templates (flexible models) which take into account both variations in shape and grey-level appearance.

In this paper, we extract two types of features from face images in order to recognize facial expressions (Sect. 2). The first type is the geometric positions of a set of fiducial points on a face. The second type is a set of multi-scale and multi-orientation Gabor wavelet coefficients extracted from the face image at the fiducial points. They can be used either independently or jointly. The architecture we developed is based on a two-layer perceptron (Sect. 3). The recognition performance with different types of features will be compared in Sect. 4. Since the first layer of the perceptron actually performs a nonlinear reduction of the dimensionality of the feature space, we will also study the desired number of hidden units, i.e., the appropriate dimension to represent a facial expression in order to achieve a good recognition rate. The importance of each individual fiducial point to facial expression recognition is studied in Sect. 5 through sensitivity analysis. Finally, we investigate the significance of image scales for facial expression recognition in Sect. 6.

The use of Gabor waveletts was motivated by the study of Lyons et al. [16]. Through the analysis based on nonmetric multidimensional scaling (nMDS) [25], Lyons et al. show that there exists a significant similarity between Gabor coding and human ratings for facial expressions. We also note that a similar representation of faces has been developed in Wiskott et al. [27] for face recognition, where they use a labeled graphs, based on a Gabor wavelet transform, to represent faces, and face recognition is done through elastic graph matching.

2. Data Set and Representation

The database we use in our experiments contains 213 images of female facial expressions. They were collected by Kamachi and Gyoba at Kyushu University, Japan. Ten expressors were asked to pose several different facial expressions. Each expressor, when ready, took pictures of herself, through remote control, while looking towards the camera through a semi-reflective plastic sheet. Original images have been rescaled and cropped such that the eyes are roughly at the same position with a distance of 60 pixels in the final images (resolution: 256 pixels $\times$ 256 pixels). The number of images corresponding to each of the 7 categories of expression (neutral, happiness, sadness, surprise, anger, disgust and fear) is roughly the same. A few of them are shown in Fig. 1. For details on the collection of these images, the reader is referred to [16].

Each image is represented in two ways. The first uses 34 fiducial points as shown in Fig. 2. They have been selected manually. Development of a technique for automatically extracting these points is under way. This is a not-yet-completely-solved solved problem, and a technique for building a similar representation has been reported in the literature [13, 27]. The image coordinates of these points (geometric positions) will be used as features in our study. Therefore, each image is represented by a vector of 68 elements.

The second way is to use features extracted with 2-D Gabor transforms [6, 15]. A 2-D Gabor function is a plane wave with wavevector $\mathbf{k}$, restricted by a Gaussian envelope function with

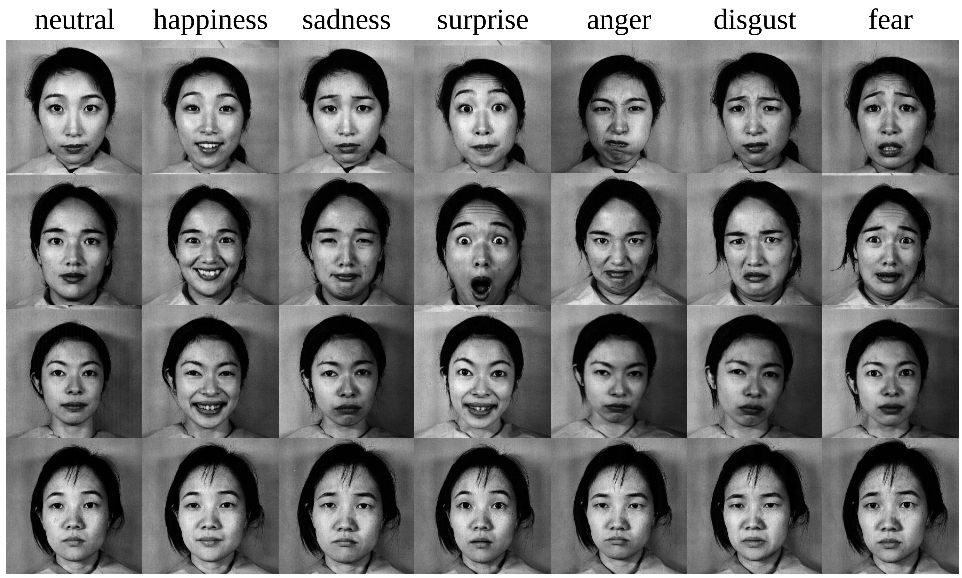

Figure 1. Facial expression database: Examples

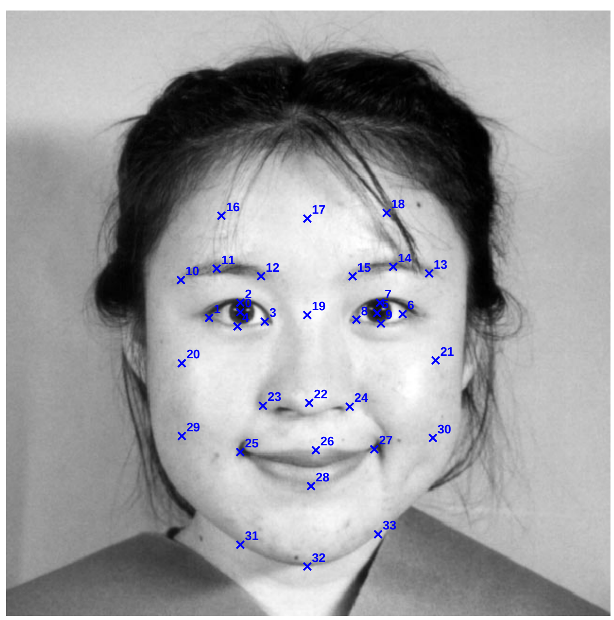

Figure 2. Geometric representation: 34 fiducial points to represent the facial geometry

relative width σ:

$$\Psi(\mathbf{k}, \mathbf{x}) = \frac{\mathbf{k}^2}{\sigma^2} \exp\left(-\frac{\mathbf{k}^2\mathbf{x}^2}{2\sigma^2}\right) \left[\exp(i\mathbf{k} \cdot \mathbf{x}) - \exp(-\frac{\sigma^2}{2})\right]$$

We set $\sigma = \pi$ for our 256×256 images. We use a discrete set of Gabor kernels which comprise 3 spatial frequencies, i.e., scales, (with wavenumber $k = \|\mathbf{k}\| = (\pi/4, \pi/8, \pi/16)$ in inverse pixels) and 6 distinct orientations from 0° to 180°, differing in 30° steps. Each image is convolved with both even and odd Gabor kernels at the location of the fiducial points as shown in Fig. 2. We have therefore 18 complex Gabor wavelet coefficients at each fiducial point. In our study, only the magnitudes are used, because they vary slowly with the position while the phases are very sensitive. In summary, with Gabor wavelet coefficients, each image is represented by a vector of 612 (18×34) elements.

3. The Architecture and Training

The architecture of our FER system is based on a two-layer perceptron (see Fig. 3). As described in Sect. 2, an image is first preprocessed, and two sets of features (geometric positions and Gabor wavelet coefficients) are extracted. These features are fed in the input units of the two-layer perceptron. The objective of the first layer is to perform a nonlinear reduction of the dimensionality of feature space, depending on the number of hidden units. Note that there are no interconnections in the first layer between geometric and Gabor-wavelet parts, because they are two pieces of information very different in nature. The second layer makes a statistical decision based on the reduced set of features in the hidden units. An output unit is associated with a particular facial expression, so our system contains 7 output units. Each output unit gives an estimate of the probability of the input image belonging to the associated facial expression.

The FER problem is considered as a statistical classification problem. The training is done by

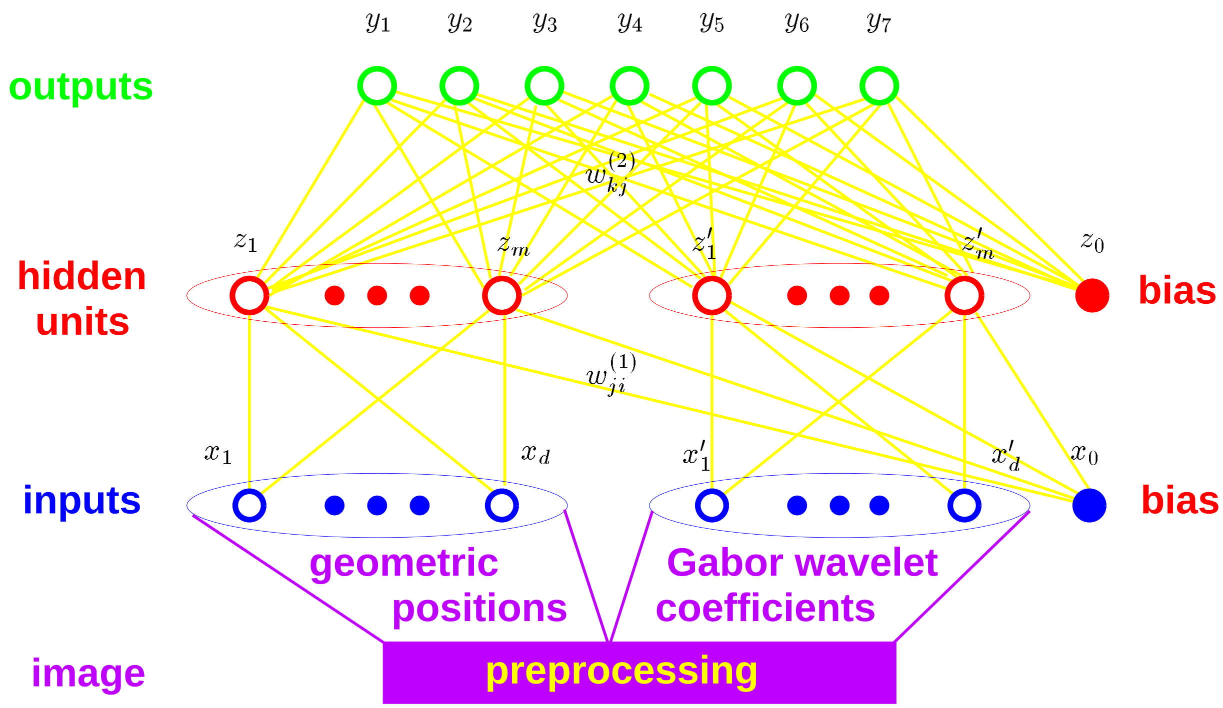

Figure 3. The architecture: There are no interconnections in the first layer between geometric and Gabor-wavelet parts

minimizing the cross-entropy for multiple classes [3]:

$$E = -\sum_n \sum_{k=1}^{c} t_k^n \ln\left(\frac{y_k^n}{t_k^n}\right) \tag{1}$$

where t_k^n and y_k^n are respectively the pattern target value and network output value, representing the probability that input $\mathbf{x}^n$ belongs to class $\mathcal{C}_k$. The error function (1) is non-negative, and reaches the absolute minimum, which is equal to zero, when $y_k^n = t_k^n$ for all k and n, i.e., when the perceptron outputs the same value as the target for each pattern. The activation function of the output units is the *softmax* function:

$$y_k = \frac{\exp(a_k)}{\sum_{k'=1}^{c} \exp(a_{k'})} \tag{2}$$

where $a_k = \sum_j w_{kj} z_j$ and z_j is the output of hidden unit j. This is the soft version of the *winner-takes-all* activation model in which the unit with the largest input has output $+1$ while all other units have output 0. The hidden units use the widely adopted 'tanh' activation function:

$$z_j = g(a_j) = \tanh(a_j) \equiv \frac{e^{a_j} - e^{-a_j}}{e^{a_j} + e^{-a_j}} \tag{3}$$

where $a_j = \sum_i w_{ji} x_i$ and x_i is the value of input unit i.

The two-layer perceptron is trained through Rprop (Resilient propagation) [21], which is a local adaptive learning scheme, performing supervised batch learning. The idea is to eliminate the harmful influence of the size of the partial derivative on the weight step. In consequence, the weight update depends only the sign of the derivative, and is exclusively determined by a weight-specific, so-called "update-value" $\Delta_{ij}^{(t)}$:

$$\Delta w_{ij}^{(t)} = \begin{cases} -\Delta_{ij}^{(t)} & \text{if } \frac{\partial E}{\partial w_{ij}}^{(t)} > 0 \\ +\Delta_{ij}^{(t)} & \text{if } \frac{\partial E}{\partial w_{ij}}^{(t)} < 0 \\ 0 & \text{otherwise} \end{cases}$$

where $\frac{\partial E}{\partial w_{ij}}^{(t)}$ denotes the summed gradient information over all patterns of the pattern set. Therefore, we increase a weight by its update-value if that direction contributes to the reduction of the overall error E, and decrease it, otherwise. The update-value $\Delta_{ij}^{(t)}$ itself is adapted based on a sign-dependent learning process:

$$\Delta_{ij}^{(t)} = \begin{cases} \eta^+ * \Delta_{ij}^{(t-1)} & \text{if } \frac{\partial E}{\partial w_{ij}}^{(t-1)} * \frac{\partial E}{\partial w_{ij}}^{(t)} > 0 \\ \eta^- * \Delta_{ij}^{(t-1)} & \text{if } \frac{\partial E}{\partial w_{ij}}^{(t-1)} * \frac{\partial E}{\partial w_{ij}}^{(t)} < 0 \\ \Delta_{ij}^{(t-1)} & \text{otherwise} \end{cases}$$

where $0 < \eta^- < 1 < \eta^+$. In words, each time the partial derivative of the corresponding weight

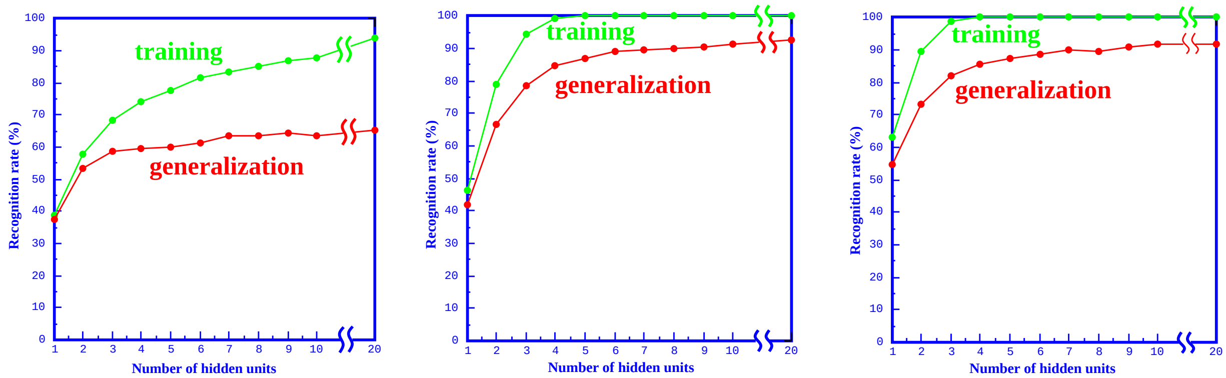

(a) Geometric positions (b) Gabor coefficients (c) Combined information

Figure 4. Recognition rate with respect to the number of hidden units

w_{ij} changes its sign, indicating that the last uodate was too big and that the algorithm has jumped over a local minimum, the update-value $\Delta_{ij}^{(t)}$ is decreased by the factor η^-; otherwise, it is slightly increased by a factor η^+ in order to accelerate convergence. We use $\eta^- = 0.5$, $\eta^+ = 1.2$.

4. Experiments on the number of hidden units

4.1. Computer Recognition Results

Our goal is to develop a recognition system which not only works well on the training data but also gives good predictions for new data. Since the size of our database is limited (213 images), we use the cross-validation technique to test different configurations of our FER architecture. Cross-validation technique is a variant of the test protocols (Jack Knife) used in statistical classification [8]. Many people have used it in order to improve the statistical reliabilities of the tests in general [3] and in face recognition in particular [7], More precisely,

- We partition the data set at random into S distinct segments (we set $S = 10$).
- We then train a two-layer perceptron using data from $S - 1$ of the segments and test its performance, by evaluating the error function (recognition rate), using the remaining segment.

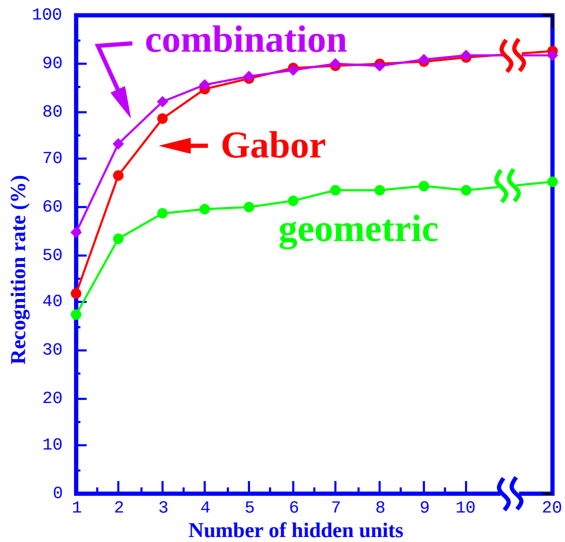

Figure 5. Comparison of the generalized recognition rates

- The above process is repeated for each of the S possible choices of the segment to be omitted from the training process.
- Finally, we average the results over all S trained two-layer perceptrons.

Since the training is a nonlinear optimization problem, the final result depends on the initial guess of the weights of the perceptrons. So, each perceptron is furthermore trained ten times with randomly initialized weights. Thus, the result for each configuration shown below is the average of the results produced by 100 trained two-layer perceptrons.

We have carried out experiments on the FER using the developed architecture by using geometric positions alone, using Gabor wavelet coefficients alone, and by using the combination of the two pieces of information. In order to investigate the appropriate dimension to code the facial expression, we vary the number of hidden units from 1 to 20. The perceptrons with geometric positions alone were trained by running 250 cycles through all the training data, while other perceptrons were trained by running only 100 cycles. The recognition rates on the training data and on the test data (generalization) with respect to the number of hidden units are shown in Fig. 4. For comparison, the generalized recognition rates of the three configurations are displayed in

Label: Surprise

NN outputs	
Neu.	0.000
Hap.	0.000
Sad.	0.000
Sur.	1.000
Ang.	0.000
Dis.	0.000
Fear	0.000

Label: Happiness

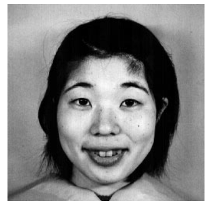

NN outputs	
Neu.	0.122
Hap.	0.720
Sad.	0.000
Sur.	0.000
Ang.	0.000
Dis.	0.000
Fear	0.158

Label: Disgust

NN outputs	
Neu.	0.001
Hap.	0.000
Sad.	0.428
Sur.	0.000
Ang.	0.016
Dis.	0.555
Fear	0.000

Label: Fear

NN outputs	
Neu.	0.002
Hap.	0.000
Sad.	0.022
Sur.	0.000
Ang.	0.001
Dis.	0.005
Fear	0.970

Figure 6. Examples of correct labeling

Fig. 5.

From the experimental results, we have the following observations:

- Gabor coefficients are much more powerful than geometric positions;
- At least two hidden units are necessary to code reasonably facial expressions;
- Probably from 5 to 7 hidden units are sufficient to code precisely facial expressions;
- Adding geometric positions improves the recognition rate only for low dimensional coding (with less than 5 hidden units). No improvement is observed when 5 or more hidden units are used.

The recognition rate (i.e., the agreement with the labeling provided by the expressors) achieved by our system is 90.1% with 7 hidden units. This should be compared with the agreement between human subjects and expressors' labeling. In the study of Lyons et al. [16], 60 human non-expert subjects were asked to rate each facial image for content of the six basic facial expressions. In 20.5% of all cases, the category which received the highest rating (averaged over all

Label: Anger

NN outputs	
Neu.	0.000
Hap.	0.000
Sad.	0.091
Sur.	0.000
Ang.	0.224
Dis.	0.685
Fear	0.000

Label: Fear

NN outputs	
Neu.	0.010
Hap.	0.000
Sad.	0.502
Sur.	0.000
Ang.	0.001
Dis.	0.007
Fear	0.479

Label: Sadness

NN outputs	
Neu.	0.099
Hap.	0.846
Sad.	0.052
Sur.	0.000
Ang.	0.000
Dis.	0.002
Fear	0.002

Label: Happiness

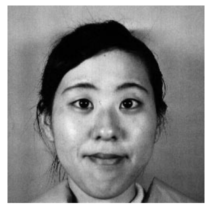

NN outputs	
Neu.	0.822
Hap.	0.017
Sad.	0.150
Sur.	0.011
Ang.	0.000
Dis.	0.000
Fear	0.000

Figure 7. Examples of disagreement

subjects) disagreed with the expression label of the image. This is similar to the results reported in the literature but with different image database [2, 14]. Several sources of this disagreement may be identified. The expressor may have posed the expression inaccurately or even incorrectly in some cases. The experimental subjects may have confused one expression with another when performing the rating task (for example, fear may be confused with surprise and anger with disgust). Therefore, the agreement between the computer (i.e., our technique) and the expressors is higher than that between the human subjects and the expressors.

In order to give the reader a concrete feeling of the FER results, we show a few examples in Fig. 6 and Fig. 7. The original labeling in the database and our system outputs are both shown. Note that, our system provides the probability it believes that an image belongs to each of the facial expression classes. The examples shown in Fig. 6 have obtained a consistent labeling from our system, while for those in Fig. 7, our system does not agree with the labeling given in the database. Note that even in the latter case, our system usually (except the last example in Fig. 7) gives a reasonable result, because the expressor may have posed an incorrect expression.

4.2. Experiments After Excluding Fear Images

The expressors found it most difficult to pose fear expressions accurately. In addition, human has more difficulty in recognizing fear. There is some evidence supporting the hypothesis that fear expressions are processed differently from the other basic facial expressions [1]. If we exclude the fear images from the database, an experiment with 30 human non-experts shows that in 85.6% of all cases, human subjects agree with the expressors' labeling, about 6% higher than when fear images are included. Hence, we have repeated exactly the same analysis as in the last subsection but with a dataset in which all fear images were excluded. The results are shown in Fig. 8. The same general observations can be made. When 7 hidden units are used, our system achieves a generalized recognition rate of 73.3% with geometric positions alone, 92.2% with Gabor wavelet coefficients alone, and 92.3% with combined information, all higher than when fear images are included (63.5%, 89.6% and 90.1%, respectively; see Fig. 5).

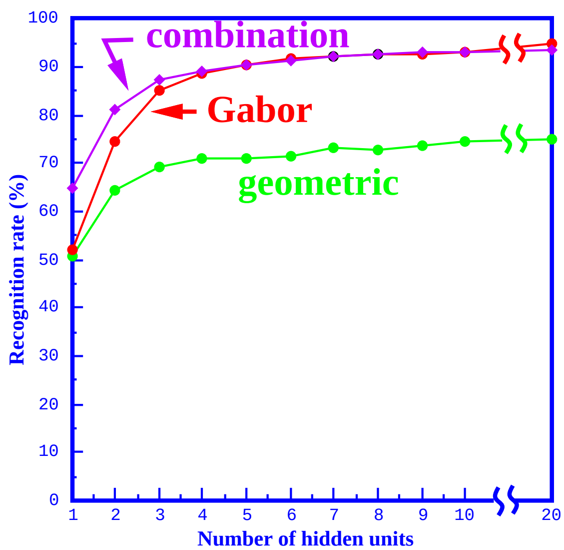

Figure 8. Comparison of the generalized recognition rates when the fear images have been excluded from the database

5. Sensitivity Analysis of Individual Fiducial Points

In this section, we shall study the importance of each fiducial point. We have used 34 fiducial points together with their Gabor wavelet coefficients. It is conceivable that each point does not play the same role, e.g., the points on the cheek should not be very informative.

This study is important for several reasons. First, by removing the least important points, i.e., by reducing the dimension of the input space, the computational cost for training and executing the multilayer perceptron is reduced. Second, the cost for extracting the fiducial points from images is reduced. Furthermore, the points on the cheek, for example, are difficult to locate precisely in the image. Third, too many input variables with respect to the training sample size can harm the performance of a sample discriminant rule. This has been noted by a number of researchers and practitioners in statistical data analysis [11, 18, 3].

The commonly used technique for dimensionality reduction is the principal component analysis (PCA), which is a linear technique. It does reduce the redundancy between the input variables, but has a big drawback: this dimensionality reduction is not related to the task at hand (in our case, FER). Big variation will be retained even though it is not informative for discriminating different classes. For example, the points on the cheek are difficult to locate precisely in the images, and therefore, there will be a large variation in the image coordinates. That variation is, however, not useful for facial expression recognition. On the other hand, the first layer of our multilayer perceptron also performs reduction of dimensionality, but the reduction is nonlinear and is related to the discrimination power of the features. This nonlinear dimensionality reduction is thus preferable over the PCA.

We are now more interested in the reduction of the number of fiducial points. We follow the approach of sensitivity analysis. If an input variable is important in FER, removing it will cause a significant change in the output, i.e., the derivative of the error function with respect to that input should be high. In our case, we have a feature vector as input for each fiducial point. Let $\mathbf{x}^{(p)}$ be the feature vector of point p and $x_i^{(p)}$ be its i^{th} element. We compute the gradient of the error function E, see (1), with respect to $\mathbf{x}^{(p)}$ as follows:

$$G^{(p)} = \left\| \frac{\partial E}{\partial \mathbf{x}^{(p)}} \right\| = \sqrt{\sum_i \left(\frac{\partial E}{\partial x_i^{(p)}} \right)^2} \tag{4}$$

where $\frac{\partial E}{\partial x_i^{(p)}}$ is the derivative of E w.r.t. $x_i^{(p)}$, to be given in Appendix A. *Points with least gradients carry little useful information for FER* , and thus can be discarded.

We have conducted exactly the same experiment as in the last section using Gabor wavelet coefficients alone. The cross-validation technique was used. Our multilayer perceptron was trained with a subset of data, while the gradient for each fiducial point was computed over an independent subset of data. The results with 4, 7 and 10 units in the hidden layer are shown in Table 1. As in the last section, the gradient value shown is also the average of 100 trials. In the table, we also provide the order of the fiducial points according to the gradient values: a point with order 0 has the largest gradient value; a point with order 33 has the least gradient value. We can observe that the ordering is quite consistent for all three configurations of the perceptron. For more direct interpretation, the result with 7 hidden units is visualized in Fig. 9, where the size of a fiducial point is proportional to the magnitude of its gradient.

Without ambiguity, the gradients of the following 10 points: 16, 17, 18, 19, 20, 21, 23, 24, 30 and 13, are much lower than the others. The gradients of points 29 and 3 are in the middle. They are mainly located on the forehead and on the cheeks. This is in accordance with our intuition: These points are hardly detectable, and therefore should carry less information for facial expression recognition. In order to validate the sensitivity analysis, we have discarded the Gabor wavelet coefficients of the above 12 points (therefore, there are only 396, instead of 612, input variables), and have again carried out the same experiment with different hidden units in the perceptron. The recognition rates on the test data (generalization) is shown in Fig. 10.

For comparison, we also show in Fig. 10 the recognition result with all 34 points. We can observe that *the generalization performance slightly improves* after discarding the 12 selected points. This is a consequence of the curse of dimensionality, as mentioned at the beginning of

	4 hidden units		7 hidden units		10 hidden units	
point	gradient	order	gradient	order	gradient	order
0	10.1936	6	7.16990	6	7.10371	6
1	13.2709	2	10.1341	2	9.93258	2
2	8.91257	8	5.67114	12	5.44258	10
3	2.21135	23	1.59910	23	1.73419	22
4	15.0430	0	10.6303	1	11.2302	0
5	4.53752	17	3.17509	19	3.01152	18
6	6.49699	13	6.07363	9	5.36752	11
7	14.9471	1	12.3932	0	10.7255	1
8	9.86957	7	6.44077	8	6.66844	7
9	5.58424	15	4.34609	15	4.34949	14
10	10.7874	3	9.02400	3	7.87800	3
11	10.3298	4	7.26315	5	7.25060	5
12	8.07026	10	5.82878	10	4.78980	13
13	0.56904	28	0.52836	27	0.52070	27
14	6.26436	14	4.84604	14	5.20799	12
15	6.80303	12	5.69166	11	4.05288	15
16	1.10122	25	0.89122	24	0.77384	25
17	0.38146	33	0.31891	33	0.31392	32
18	0.39930	32	0.32449	32	0.29637	33
19	0.45715	31	0.42730	30	0.39825	31
20	0.65773	27	0.49084	29	0.49225	29
21	0.52754	29	0.49871	28	0.49635	28
22	3.20007	20	3.96846	16	4.00260	16
23	0.66839	26	0.54490	26	0.54891	26
24	1.18916	24	0.82790	25	0.87368	24
25	4.10041	18	3.34998	18	2.52657	20
26	8.89627	9	6.67880	7	6.27436	8
27	2.92703	21	2.47474	20	2.06146	21
28	7.36040	11	5.60849	13	5.88586	9
29	2.83694	22	1.96330	22	1.72370	23
30	0.48233	30	0.38853	31	0.39990	30
31	3.49026	19	2.47427	21	2.64163	19
32	10.2121	5	8.16229	4	7.40998	4
33	4.69870	16	3.84180	17	3.50682	17

Table 1. Gradients of the error function with respect to the inputs

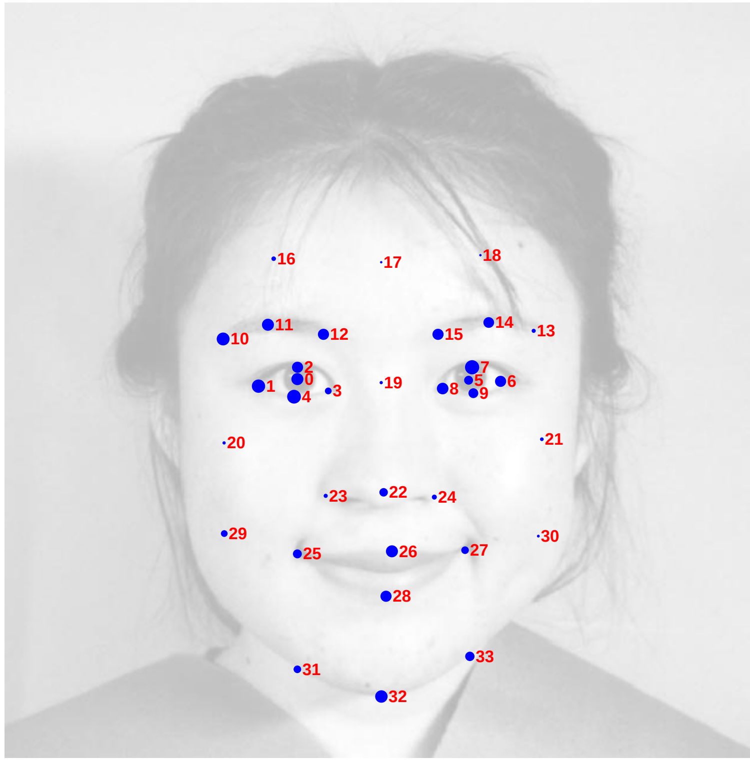

Figure 9. Importance of each fiducial point according to sensitivity analysis. The importance is illustrated by the size of a point.

this section [3]. A network with fewer inputs has fewer weights to be determined, and they are more likely to be properly constrained by a data set of *limited size*, leading to a network with better generalization properties.

As one reviewer pointed out, most expressions are mirror symmetric. However, we observe some significant difference between several symmetric points, for example, between points 10 and 13, and between points 3 and 8. There are two reasons. The first is due to the hair style variation among people. In that case, points such as 13 do not carry as consistent information as their symmetric counterparts (point 10 in this case). The second is because the facial expression is mainly a low frequency signal, as we will show in the next section. Nearby points therefore tend to be correlated, and one point (say, point 4) may carry sufficient information for facial expression recognition, making the other point (point 3 in this case) less important. Correlation

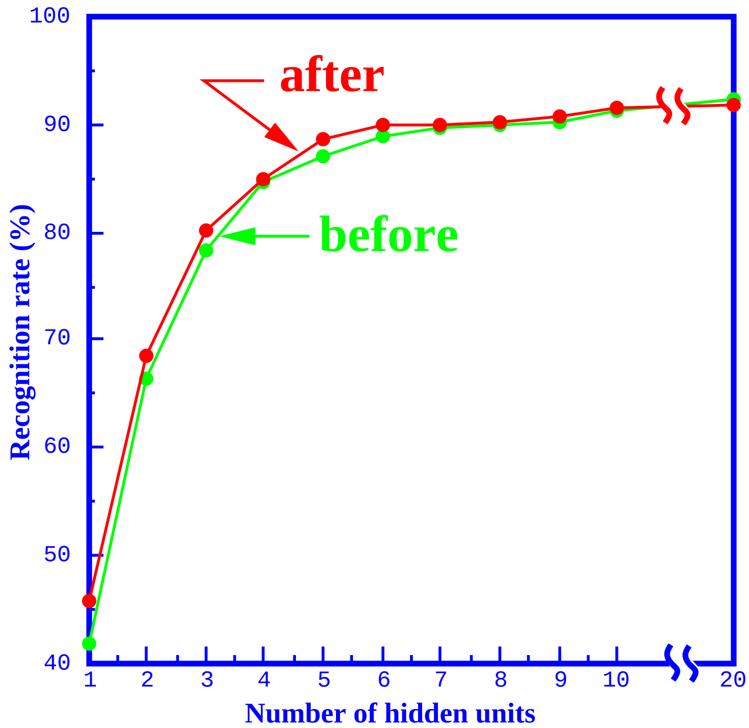

Figure 10. Comparison between the generalized recognition rates before and after deletion of the 12 points selected through sensitivity analysis

between points is one subject of our future research.

6. Significance of Image Scales

In the above experiments, we have conducted experiments on facial expression recognition using Gabor wavelets extracted from three image scales. It is conceivable that the Gabor wavelet coefficients at each image scale does not play the same role, which is the objective of this section.

We will study the significance of each spatial frequency (i.e., image scale). Besides the three spatial frequencies we used before (i.e., wavenumber $k = (\pi/4, \pi/8, \pi/16)$ in inverse pixels), we also consider one more higher scale ($k = \pi/2$) and one more lower scale ($k = \pi/32$). For simplicity, we will call $k = \pi/32, \pi/16, \pi/8, \pi/4$ and $\pi/2$ *scale 1, 2, 3, 4 and 5*, respectively. That is, scale 1 corresponds to the lowest spatial frequency ($k = \pi/32$); scale 5 corresponds to the highest spatial frequency ($k = \pi/2$). We have performed exactly the same type of experiments as in Sect. 4 by using the Gabor wavelet coefficients of only one particular image scale (The fear images are included). The results of the generalized recognition rates with respect to the number of hidden units are shown in Fig. 11. A subset of the results, corresponding to 7 hidden units, is shown in Fig. 12. It is clear that facial expression recognition by computer is mainly a low spatial frequency process. In particular, scales 2 and 3 are most significant to the recognition. Recall that the images we use have a spatial resolution of 256 pixels $\times$ 256 pixels. Therefore, the above result of our study reveals that a resolution of *64 pixels* $\times$ *64 pixels* or lower is probably enough for facial expression recognition, which is in accordance of the general belief that a resolution of 16 pixels $\times$ 16 pixels is the minimum resolution that allows face identification [12].

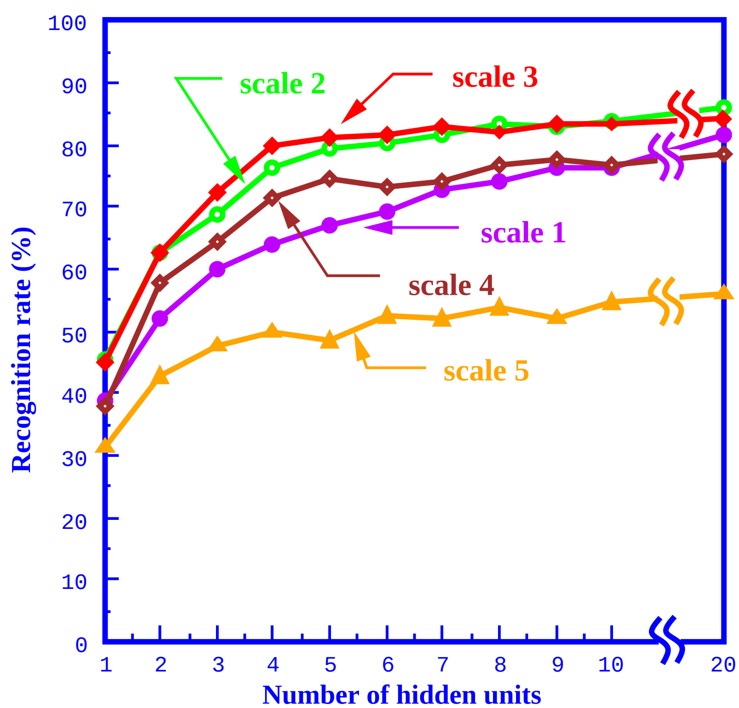

Figure 11. Generalized recognition rates of different image scales with respect to the number of hidden units

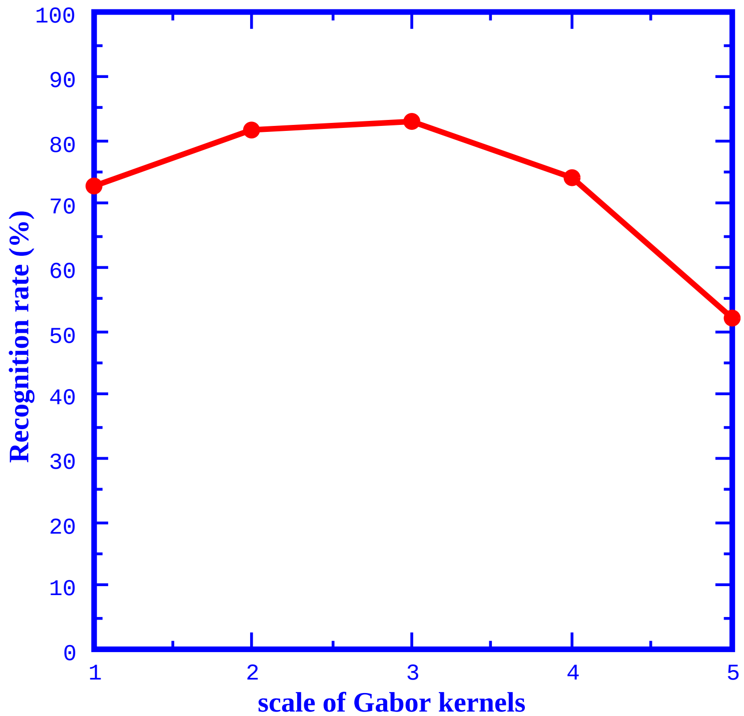

Figure 12. Generalized recognition rates with respect to image scales for 7 hidden units

7. Conclusion

In this paper, we have developed an architecture based on a two-layer perceptron for recognizing facial expressions. We have first compared the use of two types of features extracted from face images. The first type is the geometric positions of a set of fiducial points on a face. The second type is a set of multi-scale and multi-orientation Gabor wavelet coefficients extracted from the face image at the fiducial points. They can be used either independently or jointly. Comparison of the recognition performance with different types of features shows that Gabor wavelet coefficients are much more powerful than geometric positions and that the agreement between computer and the expressors' labeling is higher than that between human subjects and the expressors' labeling.

Furthermore, since the first layer of the perceptron actually performs a nonlinear reduction of the dimensionality of the feature space, we have also studied the desired number of hidden units, i.e., the appropriate dimension to represent a facial expression in order to achieve a good recognition rate. It turns out that at least two hidden units are necessary to code reasonably facial expressions and that five to seven hidden units are probably enough to give a precise representation.

Then, we have investigated the importance of each individual fiducial point to facial expression recognition. Sensitivity analysis reveals that points on cheeks and on forehead carry little useful information. After discarding them, not only the computational efficiency increases, but also the generalization performance slightly improves. This has an important consequence: we only need to extract features in the eyes and mouth regions from images. Note that we have only studied the sensitivity of each individual fiducial point on a face. There may exist strong correlations between the features of some points such as those on both eyes. This is one subject of our future research.

Finally, we have studied the significance of image scales. Experiments show that facial expression recognition is mainly a low frequency process, and a spatial resolution of 64 pixels $\times$ 64 pixels or lower is probably enough.

Acknowledgment

Part of this work was done when the author was on sabbatical at ATR (Advanced Telecommunications Research Institute International), Kyoto, Japan, in 1997. The draft version of this paper was prepared when the author was still employed at INRIA Sophia-Antipolis, France. Michael Lyons, Michael Schuster, and Shigeru Akamatsu (all from ATR, Japan) have contributed to the initial stage of the work. The author thanks Miyuki Kamachi and Jiro Gyoba (Kyushu University, Japan) for providing the facial expression database, and Michael Lyons for computing the Gabor wavelet coefficients. The author appreciates the comments from the reviewers.

A Derivative Evaluation

We now calculate $\partial E/\partial x_i$, the derivative of the error function E given in (1) with respect to the input variable x_i. The error function (1) can be rewritten as

$$E = \sum_n E^n \qquad \text{with} \quad E^n = -\sum_{k=1}^{c} t_k^n \ln\big(\frac{y_k^n}{t_k^n}\big) \tag{5}$$

Then,

$$\frac{\partial E}{\partial x_i} = \sum_n \frac{\partial E^n}{\partial x_i} \tag{6}$$

Using the chain rule for partial derivatives, we have

$$\frac{\partial E^n}{\partial x_i} = \sum_{k=1}^{c} \frac{\partial}{\partial y_k}\left[-t_k^n \ln\big(\frac{y_k^n}{t_k^n}\big)\right]\frac{\partial y_k}{\partial x_i} = -\sum_{k=1}^{c} \frac{t_k^n}{y_k}\frac{\partial y_k}{\partial x_i} \tag{7}$$

where the summation runs over all output units, and y_k is the softmax function (2). Note that y_k depends on input x_i via the hidden units. By applying the chain rule, the derivative of output y_k with respect to input x_i, $\partial y_k/\partial x_i$, is computed as follows:

$$\frac{\partial y_k}{\partial x_i} = \sum_{j=1}^{m} \frac{\partial y_k}{\partial a_j}\frac{\partial a_j}{\partial x_i} = \sum_{j=1}^{m} w_{ji}^{(1)}\frac{\partial y_k}{\partial a_j} \tag{8}$$

where the summation runs over all units in the hidden layer. The evaluation of $\partial y_k/\partial a_j$ can be done in a recursive way:

$$\begin{aligned}\frac{\partial y_k}{\partial a_j} &= \sum_{k'=1}^{c} \frac{\partial y_k}{\partial a_{k'}}\frac{\partial a_{k'}}{\partial a_j} = \sum_{k'=1}^{c} \frac{\partial y_k}{\partial a_{k'}}\left[g'(a_j)w_{k'j}^{(2)}\right] \\ &= g'(a_j)\sum_{k'=1}^{c} w_{k'j}^{(2)}\frac{\partial y_k}{\partial a_{k'}}\end{aligned} \tag{9}$$

where $g'(a_j)$ is the first derivative of the activation function (3), and from (2), $\partial y_k / \partial a_{k'}$ is given by

$$\frac{\partial y_k}{\partial a_{k'}} = y_{k'} \delta_{kk'} - y_{k'} y_k \tag{10}$$

where $\delta_{kk'}$ is the Kronecker delta symbol, and is equal to 1 if $k = k'$ and 0 otherwise.

In summary, we can compute $\partial E / \partial x_i$ as follows. First, apply the input vector $\mathbf{x}^n$ of pattern n and propagate forward to obtain the activations of all of the hidden and output units in the multilayer perceptron. Second, back-propagate the derivatives $\frac{\partial y_k}{\partial a_j}$ according to the recursive formula (9), starting with (10), for all hidden units. Third, back-propagate to the inputs to obtain the derivative $\partial y_k / \partial x_i$ using (8). The second and third steps are repeated for each output y_k and each input x_i. Finally, $\partial E^n / \partial x_i$ is calculated using (7). Repeat the above procedure for all patterns and use (6) to compute $\partial E / \partial x_i$.

References

[1] R. Adolphs, D. Tranel, H. Damasio, and A. Damasio. Impaired recognition of emotion in facial expressions following bilateral damage to the human amygdala. *Nature*, 372:669–672, 1994.

[2] M. Bartlett, P. Viola, T.Sejnowski, L. Larsen, J. Hager, and P. Ekman. Classifying facial action. In D. Touretzky, M. Mozer, and M. Hasselmo, editors, *Advances in Neural Information Processing Systems 8*. MIT Press, Cambridge, MA, 1996.

[3] C. Bishop. *Neural Networks for Pattern Recognition*. Clarendon Press, Oxford, 1995.

[4] R. Chellappa, C. Wilson, and S. Sirohey. Human and machine recognition of faces: A survey. *Proceedings of the IEEE*, 83(5):705–740, May 1995.

[5] G. Cottrell and J. Metcalfe. Face, gender and emotion recognition using holons. In D. Touretzky, editor, *Advances in Neural Information Processing Systems 3*, pages 564–571. Morgan and Kaufman, San Mateo, 1991.

[6] J. Daugman. Complete discrete 2-D Gabor transforms by neural networks for image analysis and compression. *IEEE Transactions on Acoustic, Speech and Signal Processing*, 36(7):1169–1179, July 1988.

[7] B. Duc, G. Maître, S. Fischer, and J. Bigun. Person authentication by fusing face and speech information. In J. Bigun, G. Chollet, and G. Borgefors, editors, *Audio and Video Based Person Authentication - AVBPA97*, volume LNCS-1206, pages 311–318. Springer, 1997.

[8] B. Efron and R. Tibshirani. *An introduction to the Boostrap*. Chapman & Hall, New York, 1993.

[9] P. Ekman and W. Friesen. *Unmasking the Face: A guide to recognizing emotions from facial expressions*. Consulting Psychologists Press, Palo Alto, CA, 1975.

[10] I. Essa and A. Pentland. Coding, analysis, interpretation, and recognition of facial expressions. *IEEE Transactions on Pattern Analysis and Machine Intelligence*, 19(7):757–763, July 1997.

[11] R. Gnanadesikan. *Methods for Statistical Data Analysis of Multivariate Observations*. Wiley Series in Probability and Statistics. Wiley, New York, 2nd edition, 1997.

[12] L. Harmon. The recognition of faces. In R. Held, editor, *Image, Object, and Illusion*, Readings from Scientific American, chapter 10, pages 101–112. W.H. Freeman and Company, San Francisco, 1974.

[13] M. Lades, J. Vorbrüggen, J. Buhmann, J. Lange, C. von der Malsburg, R. Wurtz, and W. Konen. Distortion invariant object recognition in the dynamic link architecture. *IEEE Transactions on Computers*, 42(3):300–311, 1993.

[14] A. Lanitis, C. Taylor, and T. Cootes. Automatic interpretation and coding of face images using flexible models. *IEEE Transactions on Pattern Analysis and Machine Intelligence*, 19(7):743–756, July 1997.

[15] T. Lee. Image representation using 2d Gabor wavelets. *IEEE Transactions on Pattern Analysis and Machine Intelligence*, 18(10):959–971, Oct. 1996.

[16] M. Lyons, S. Akamatsu, M. Kamachi, and J. Gyoba. Coding facial expressions with gabor wavelets. In *Proceedings of the Third IEEE International Conference on Automatic Face and Gesture Recognition*, Nara, Japan, Apr. 1998.

[17] K. Mase. Recognition of facial expression from optical flow. *IEICE Transactions E*, 74(10):3473–3483, 1991.

[18] G. McLachlan. *Discriminant Analysis and Statistical Pattern Recognition*. Wiley Series in Probability and Mathematical Statistics. Wiley, New York, 1992.

[19] C. Padgett and G. Cottrell. Identifying emotion in static images. In *Proceedings of the 2nd Joint Symposium on Neural Computation*, volume 5, pages 91–101, La Jolla, CA, 1997.

[20] A. Rahardja, A. Sowmya, and W. Wilson. A neural network approach to component versus holistic recognition of facial expressions in images. In *Intelligent Robots and Computer Vision X: Algorithms and Techniques*, volume 1607 of *SPIE Proc.*, pages 62–70, 1991.

[21] M. Riedmiller and H. Braun. A direct adaptive method for faster backpropagation learning: The RPROP algorithm. In H. Ruspini, editor, *Proceedings of the International Conference on Neural Networks*, pages 586 – 591, San Fransisco, CA, Mar. 1993.

[22] H. Rowley, S. Baluja, and T. Kanade. Human face detection in visual scenes. Technical Report CMU-CS-95-158R, School of Computer Science, Carnegie Mellon University, Nov. 1995.

[23] M. Suma, N. Sugie, and K. Fujimora. A preliminary note on pattern recognition of human emotional expression. In *Proceedings of the 4th International Joint Conference on Pattern Recognition*, pages 408–410, 1978.

[24] K.-K. Sung and T. Poggio. Example-based learning for view-based human face detection. Technical Report A.I. Memo 1521, CBCL Paper 112, MIT, Dec. 1994.

[25] T. Takane, F. Young, and J. de Leeuw. Nonmetric individual differences multidimensional scaling: An alternating least squares method with optimal scaling features. *Psychometrika*, 42:7–67, 1977.

[26] M. Turk and A. Pentland. Eigenfaces for recognition. *J. of Cognitive Neuroscience*, 3(1):71–86, Mar. 1991.

[27] L. Wiskott, J.-M. Fellous, N. Krüger, and C. von der Malsburg. Face recognition by elastic bunch graph matching. *IEEE Transactions on Pattern Analysis and Machine Intelligence*, 19(7):775–779, July 1997.

[28] Y. Yacoob and L. Davis. Recognizing facial expressions by spatio-temporal analysis. In *Proceedings of the International Conference on Pattern Recognition*, volume 1, pages 747–749, Jerusalem, Israel, Oct. 1994. Computer Society Press.